JOURNAL OF AGRICULTURAL AND FOOD CHEMISTRY

Article

Cite This: J. Agric. Food Chem. 2018, 66, 5790−5801

pubs.acs.org/JAFC

Anti-inflammatory Activity of 8-Hydroxydaidzein in LPS-Stimulated BV2 Microglial Cells via Activation of Nrf2-Antioxidant and Attenuation of Akt/NF-κB-Inflammatory Signaling Pathways, as Well As Inhibition of COX-2 Activity

Pei-Shan Wu,[†,§] Hsiou-Yu Ding,[‡,§] Jui-Hung Yen,[∥] Shu-Fen Chen,[⊥] Kuan-Han Lee,[#] and Ming-Jiuan Wu*[,†]

[†]Department of Biotechnology, [‡]Department of Cosmetic Science, [⊥]Department of Health and Nutrition, and [#]Department of Pharmacy, Chia Nan University of Pharmacy and Science, Tainan 717, Taiwan

[∥]Department of Molecular Biology and Human Genetics, Tzu Chi University, Hualien 970, Taiwan

Supporting Information

ABSTRACT: It was demonstrated that isoflavones can cross the blood−brain barrier, making them desirable candidate agents for the prevention of neurological symptoms. 8-Hydroxydaidzein (8-OHD, 4′,7,8-trihydoxyisoflavone) is an isoflavone found only in fermented soy food. Current results showed that 8-OHD inhibited LPS-stimulated production of nitric oxide (NO) and proinflammatory cytokines, such as tumor necrosis factor (TNF)-α and interleukin (IL)-6, by inhibiting gene expression in BV2 microglial cells. Moreover, 8-OHD markedly quenched reactive oxygen species (ROS) and activated NF-E2-related factor 2 (Nrf2) so as to upregulate expression of Phase II enzymes, including heme oxygenase (HO)-1, NAD(P)H quinone dehydrogenase 1 (NQO1), and the modifier subunit of glutamate cysteine ligase (GCLM). 8-OHD also suppressed LPS-stimulated phosphorylation of Akt and NF-κB-p65. The anti-inflammatory activity of 8-OHD was attenuated by the HO-1 inhibitor zinc protoporphyrin (Znpp) but augmented by the PI3K/Akt inhibitor LY294002. 8-OHD also diminished LPS-induced prostaglandin E_2 (PGE_2) production without affecting cyclooxygenase (COX)-2 expression. In vitro assay shows that 8-OHD displayed mixed-type inhibition of COX-2 with an IC_{50} of 8.9 ± 1.2 μM. These data suggest that the anti-inflammatory activity of 8-OHD may be associated with the activation of Nrf2/HO-1 and attenuation of Akt/NF-κB signaling pathways as well as inhibition of COX-2 enzyme activity. In conclusion, 8-OHD, a potent Nrf2 activator, Akt/NF-κB activation suppressor, and COX-2 enzyme inhibitor, may have health-promoting effects for mitigating microglia activation and preventing neuroinflammation.

KEYWORDS: *8-hydroxydaidzein, Nrf2, Akt, NF-κB, COX-2*

INTRODUCTION

Microglial cells are the principle resident macrophages in the central nervous system (CNS).[1] They are responsible for brain development, tissue maintenance, and repair.[2] In healthy adult CNS, quiescent resting microglia surveil the tissue, being ready to rapidly transform to activated states upon real or potential danger to the CNS.[3] Activated microglia proliferate, exert phagocytic activities, and produce immune-modulatory molecules, such as nitric oxide (NO), prostaglandin E_2 (PGE_2), proinflammatory cytokines, and reactive oxygen species (ROS).[4] They thus play a key role in neuroinflammation, which is a fundamental process in neurodegenerative diseases, such as Alzheimer's disease, Parkinson's disease, prion diseases, multiple sclerosis, and AIDS dementia.[5]

Nuclear factor E2-related factor 2 (Nrf2) and nuclear factor-κB (NF-κB) are the two key transcription factors that regulate cellular responses to oxidative stress and inflammation, respectively.[6] Nrf2 level is tightly regulated by binding to Keap1 (Kelch-like ECH-associated protein 1), which mediates Nrf2 ubiquitination and subsequent proteasomal degradation.[6] In the presence of oxidative and xenobiotic stresses, Keap1 changes conformation and prevents binding to Nrf2, leading to a rapid translocation and accumulation of Nrf2 in the nucleus. There Nrf2 forms a heterodimer with one of the small Maf proteins and binds to the antioxidant responsive elements (ARE) of target genes, which include a group of functionally diverse cytoprotective proteins, such as heme oxygenase-1 (HO-1), NAD(P)H, NAD(P)H:quinone oxidoreductase 1 (NQO1), and glutamate-cysteine ligase (GCL).[7] Small Nrf2 activators, including dietary polyphenolic compounds, have been known to attenuate inflammation and reduced risk of many chronic diseases.[8,9]

NF-κB is composed of different dimers, and a p50/p65 heterodimer is the most common one.[10] The canonical activation pathway is mediated by IκB kinase (IκKs) complex, which phosphorylates the inhibitors of NF-κB (IκBs) and leads to the proteasomal degradation of IκBs, allowing NF-κB to enter the nucleus and cause the expression of inflammatory genes. IκKs also phosphorylate the p65 subunit at Ser^{536}, which

Received: January 24, 2018
Revised: May 20, 2018
Accepted: May 23, 2018
Published: May 23, 2018

Downloaded via CHIA NAN UNIV OF PHARMACY & SCIENCE on November 20, 2019 at 06:27:20 (UTC).
See https://pubs.acs.org/sharingguidelines for options on how to legitimately share published articles.

© 2018 American Chemical Society

DOI: 10.1021/acs.jafc.8b00437
J. Agric. Food Chem. 2018, 66, 5790−5801

is involved in regulation of NF-κB nuclear translocation, transcriptional activity, and protein stability.[11] Recent studies have clearly demonstrated that the phosphatidyl inositol 3-kinase (PI3K)/Akt signal pathway is required for efficient activation of NF-κB-dependent inflammatory responses in microglial cells.[12] There are functional interactions and cross-talks between the Nrf2 and the NF-κB pathways to maintain the fine balance of cellular redox status and regulate the responses to stress and inflammation.[6]

Isoflavones are a class of dietary phytoestrogens produced almost exclusively by the members of the *Fabaceae* family. Genistein (4′,5,7-trihydroxyisoflavone), daidzein (4′,7-dihydroxyisoflavone), and glycetein (4′,7-dihydroxy-6-methoxyisoflavone) are the best known free isoflavones found in soy.[13] Due to their estrogenic activity, numerous clinical studies revealed the benefits of genistein and daidzein in the prevention of breast and prostate cancers, cardiovascular disease, and osteoporosis, as well as in relieving postmenopausal symptoms.[14,15]

Genistein (Gen, SFigure 1a), the most widely studied soy isoflavone, can cross the blood−brain barrier (BBB), making it an especially desirable potential drug for the treatment of neurodegenerative diseases.[16] It can protect cells from oxidative stress[15] and inhibit the production of proinflammatory mediators in lipopolysaccharide (LPS)-treated microglia cells[17] and in TNF-α-treated human brain microvascular endothelial cells.[18] Animal experiments show that oral administration of Gen attenuated LPS-induced cognitive impairments in rat.[19] Daidzein also penetrates to the brain through the BBB[20] and exhibits anti-inflammatory effects in β-amyloid- and LPS-activated astrocyte cells.[21]

In contrast to the above-mentioned genistein and daidzein, *ortho*-hydroxyl isoflavones are usually isolated from fermented soybean products rather than from the plant per se.[22] 8-Hydroxydaidzein (8-OHD, 4′,7,8-trihydroxyisoflavone, SFigure 1b) has recently attracted much attention due to its strong antioxidant, antitumor, antimelanogenesis, aldose reductase inhibitory, and hepatoprotective activities.[22−25] However, the anti-inflammatory effect of 8-OHD has never been studied before. We thus intended to study the inhibitory effects of 8-OHD along with its *meta*-hydroxy isomer, Gen, on the production of NO, pro-inflammatory cytokines, and PGE_2 in LPS-treated BV2 murine microglial cells. Furthermore, its effects on ROS generation and signal pathways including Nrf2, Akt, and NF-κB were also investigated.

MATERIALS AND METHODS

Chemicals. Polymyxin B (PMB), lipopolysaccharide (LPS, *Escherichia coli* O111:B4), Griess reagent, 3-[4,5-dimethylthiazol-2-yl]-2,5-diphenyl tetrazolium bromide (MTT), RIPA lysis buffer, and other chemicals were from Sigma-Aldrich Co. (St. Louis, MO), unless otherwise indicated. Genistein (purity ≥ 98%), zinc protoporphyrin-IX, and nuclear extraction kit were from Cayman Chemical (Ann Arbor, MI, USA). Mouse TNF-α and IL-6 ELISA Sets were from BD Biosciences (San Diego, CA, USA). PI3K/Akt inhibitor LY294002 was from Promega (Madison, WI). Prostaglandin E2 (PGE_2) ELISA kit was from Abcam (Cambridge, UK). Fluorometric COX-2 inhibitor screening kit was purchased from Biovision (Milpitas, CA, USA).

Isolation and Identification of 8-Hydroxydaidzein (8-OHD, 4′,7,8 -Trihydoxyisoflavone). 8-OHD was isolated from soybean fermented by *Aspergillus oryzae* according to a process described in the literature.[23] Soy fermented product (500 g) was refluxed with methanol (5 L) for 3 h to give a methanol extract (102 g). The extract was suspended in water (0.1 L), and re-extracted with hexane and ethyl acetate. Each extraction was concentrated under vacuum to give hexane (54 g), ethyl acetate (5.43 g), and water (37 g) fractions. The ethyl acetate extract was subjected to silica gel column chromatography and eluted with hexane/ethyl acetate (3:1), hexane/ethyl acetate (1:1), ethyl acetate, ethyl acetate/methanol (1:1), and methanol. The ethyl acetate fraction was further separated on a repeated HPLC using a semipreparative C-18 ODS2 OBD Prep Column (Spherisorb, 80 Å, 5 μm, 10 mm × 250 mm) according to a previous method.[26] The mobile phase consisted of elute A (0.1% v/v acetic acid in double distilled water) and elute B (acetonitrile, Merck). The elution was started with 14% v/v B for 10 min (isocratically), followed by a linear gradient of B that increased from 20% to 40% v/v over 50 min with a constant flow rate of 3 mL/min. The peak corresponding to 8-OHD was collected and lyopholized to white powder (14.7 mg). The compound was identified by mass and NMR spectrometry.

8-OHD:[24] ^{1}H NMR (DMSO-d_6) δ: 6.79 (2H, d, J = 8.3 Hz, H-3′, 5′), 6.94 (1H, d, J = 8.7 Hz, H-6), 7.37 (2H, d, J = 8.3 Hz, H-2′, 6′), 7.45 (1H, d, J = 8.7 Hz, H-5), 8.30 (1H, s, H-2), 9.46 (1 H, br. s, OH-7), 9.58 (1H, br. s, OH-4 ′), 10.37 (1H, br. s, OH-8). ^{13}C NMR (DMSO-d_6) δ: 175.6 (C-4), 157.4 (C-4′), 153.0 (C-2), 150.2 (C-7), 147.0 (C-9), 133.2 (C-8), 130.4 (C-2′, 6′), 123.2 (C-1′), 123.0 (C-3), 117.7 (C-10), 116.0 (C-5), 115.3 (C-3′, 5′), 114.5 (C-6). FAB MS, m/z 271 $[M + H]^+$.

The purity of the isolated 8-OHD was 99% determined by the single peak with retention time 2.276 min on the ultraperformance liquid chromatography (UPLC) profile (SFigure 2). UPLC was operated through an analytic C18 reversed-phase column (Acquity UPLC BEH C18, 1.7 μm, 2.1 mm × 100 mm, Waters, Milford, CT, USA) and a gradient elution using water (A) containing 1% (v/v) acetic acid and methanol (B) with a linear gradient for 5 min with 15% to 35% B at a flow rate of 0.3 mL/min.[27]

Culture of BV2 Cells. Immortalized mouse microglial cell line BV2 was kindly provided by Professor Shun-Fen Tzeng (National Cheng Kung University, Tainan, Taiwan). BV2 cells were cultured in Dulbecco's Modified Eagle Medium/Nutrient Mixture F-12 (DMEM/F12, Invitrogen Life Technologies, Carlsbad, CA, USA) with 10% fetal bovine serum (HyClone, Logan, UT, USA), 100 U/mL penicillin, and 100 μg/mL streptomycin. Cells were maintained in a humidified incubator at 37 °C in 5% CO_2.

Treatment of BV2 Cells and Measurement of Cell Viability, and Production of Nitrite, TNF-α, IL-6, and Prostaglandin E_2 (PGE_2). BV2 cells (1×10^6/mL) were pretreated with vehicle (0.1% DMSO), polymyxin B (PMB), 8-OHD, or Gen for 30 min prior to LPS insult. Culture medium was collected 20 h later for the measurement of nitrite, TNF-α, IL-6, and PGE_2, and cell viability was determined by MTT (3-(4,5-dimethylthiazol-2-yl)-2,5-diphenyltetrazolium bromide) tetrazolium reduction assay.[28]

Nitrite (NO_2^-) was determined using the Griess reagent, and A_{550} was measured against a sodium nitrite standard curve. TNF-α and IL-6 were measured by Mouse TNF-α and IL-6 ELISA Sets. PGE_2 was determined using PGE_2 ELISA kit.

RNA Extraction and Reverse Transcription Real-Time PCR. Total RNA extraction was carried out using the Illustra RNA Spin Mini RNA Isolation Kit (GE Healthcare). The reverse transcription of the RNA samples was performed using a High-Capacity cDNA Archive kit (Thermo Fisher Scientific). Quantitative PCR was performed using a Power SYBR Green PCR Master Mix (Thermo Fisher Scientific) and ABI StepOne Real Time PCR System. The reactions were performed in a total volume of 20 μL that contained 0.4 μM of each primer (STable 1). PCR conditions were 95 °C for 2 min, 40 cycles at 94 °C for 15 s, and 60 °C for 60 s. The relative mRNA expression was normalized with β-actin expression and then calculated by the $2^{-\Delta\Delta CT}$ method. The identity and purity of the amplified product was checked through analysis of the melting curve.

Preparation of Cell Lysates and Nuclear Extracts and Immunoblot Analysis. BV2 cells were washed twice with ice-cold phosphate saline buffer (pH 7.4). Total cell lysates and nuclear extracts were prepared by RIPA lysis buffer and a nuclear extraction kit, respectively. The protein concentration was determined by the

DOI: 10.1021/acs.jafc.8b00437
J. Agric. Food Chem. 2018, 66, 5790−5801

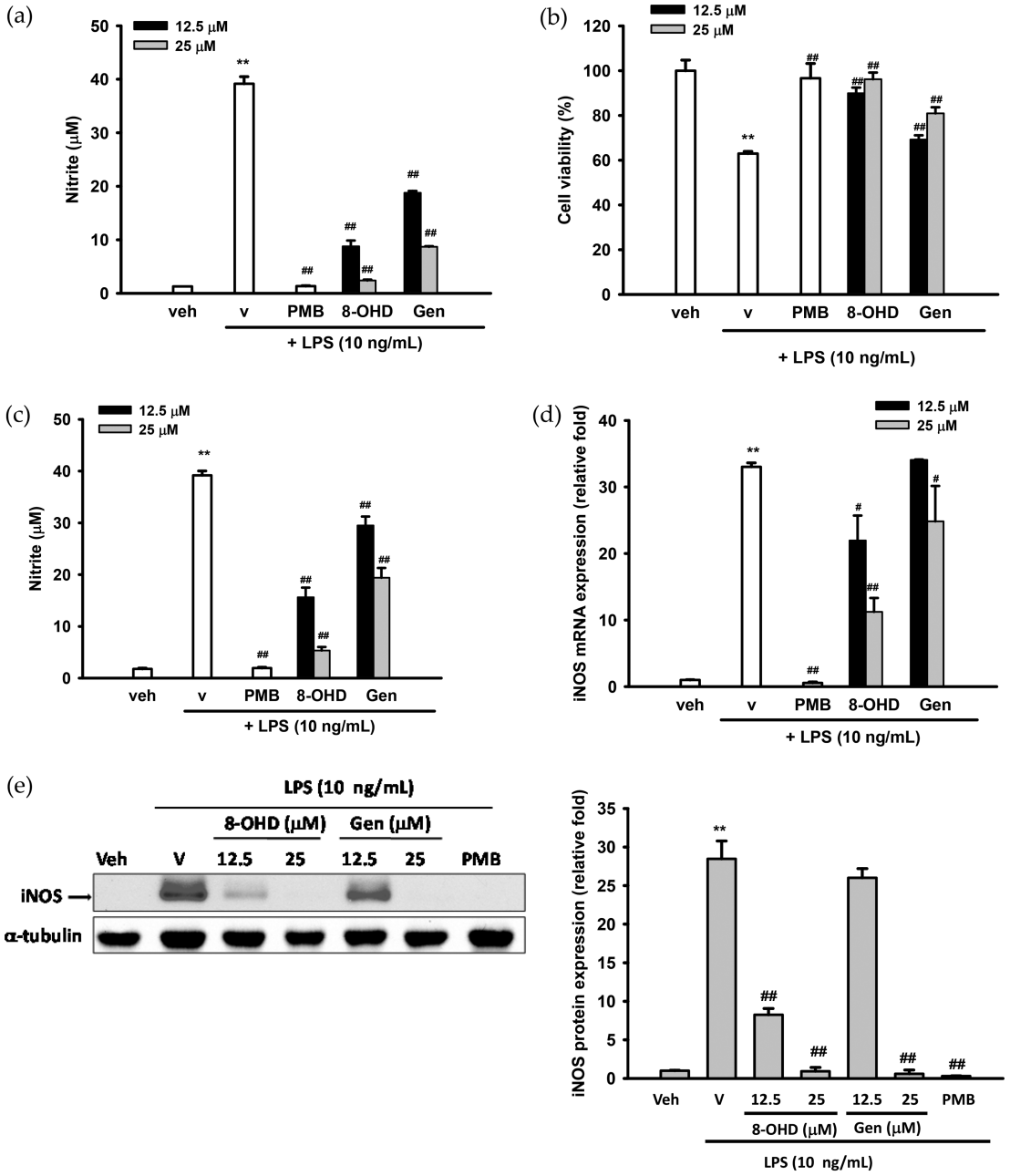

Figure 1. Effects of 8-hydroxydaidzein (8-OHD) and genistein (Gen) on lipopolysaccharide (LPS)-stimulated production of nitric oxide (NO) and iNOS expression. (a and b) 8-OHD and Gen inhibited LPS-mediated NO production and cytotoxicity. BV2 cells were pretreated for 0.5 h with vehicle (0.1% DMSO), polymyxin B (PMB, 10 μg/mL), or the indicated concentration of compound and then stimulated with LPS (10 ng/mL) for 20 h. The cell viability and production of nitrite were determined as described in the Materials and Methods. (c) Post-treatment of 8-OHD and Gen inhibited LPS-mediated NO production in BV2 cells. BV2 cells were stimulated with LPS (10 ng/mL) for 0.5 h prior to treatment of vehicle (0.1% DMSO), polymyxin B (PMB, 10 μg/mL), or the indicated concentration of compound. The nitrite production was analyzed 20 h after LPS challenge. (d) BV2 cells were pretreated with the indicated reagent for 30 min and then stimulated with LPS for 4 h. RNA was isolated, and iNOS mRNA was measured by RT-Q-PCR, as described in the Materials and Methods. (e) Total protein was prepared 16 h after LPS challenge. Protein levels of iNOS and α-tubulin were detected by Western blotting, as described in the Materials and Methods. Representative blots from one of the three independent experiments are shown. Band intensities were quantified by ImageJ software and indicated as relative folds of iNOS/α-tubulin. Data are represented as the mean ± SD (n = 3). Statistical differences are presented ** p < 0.01 compared with the vehicle control (without LPS) and # p < 0.05, ## p < 0.01 compared with the LPS-treated vehicle.

Bradford method (Bio-Rad Laboratories, Hercules, CA, USA) using bovine serum albumin as a standard reference.

Equal amounts of protein were subjected to electrophoresis by SDS/PAGE. Proteins were transferred onto polyvinylidene difluoride (PVDF) membranes (Hybond-P, GE Healthcare, Pittsburgh, PA, USA) using CAPS buffer system (10 mM CAPS pH 10.5, 10% v/v methanol) at 20 V overnight at 4 °C. The membranes were then incubated with freshly made blocking PBST buffer (5% skim milk in PBS with 0.05% v/v Tween 20, pH 7.4) for 8 h at room temperature, followed by overnight incubation with specific primary antibody (STable 2) at 4 °C. The blots were washed in PBST three times and subsequently incubated with suitable horseradish peroxidase-conjugated secondary antibody (Jackson ImmunoResearch, West Grove, PA, USA) for 1 h before enhanced chemiluminescence detection

DOI: 10.1021/acs.jafc.8b00437
J. Agric. Food Chem. 2018, 66, 5790−5801

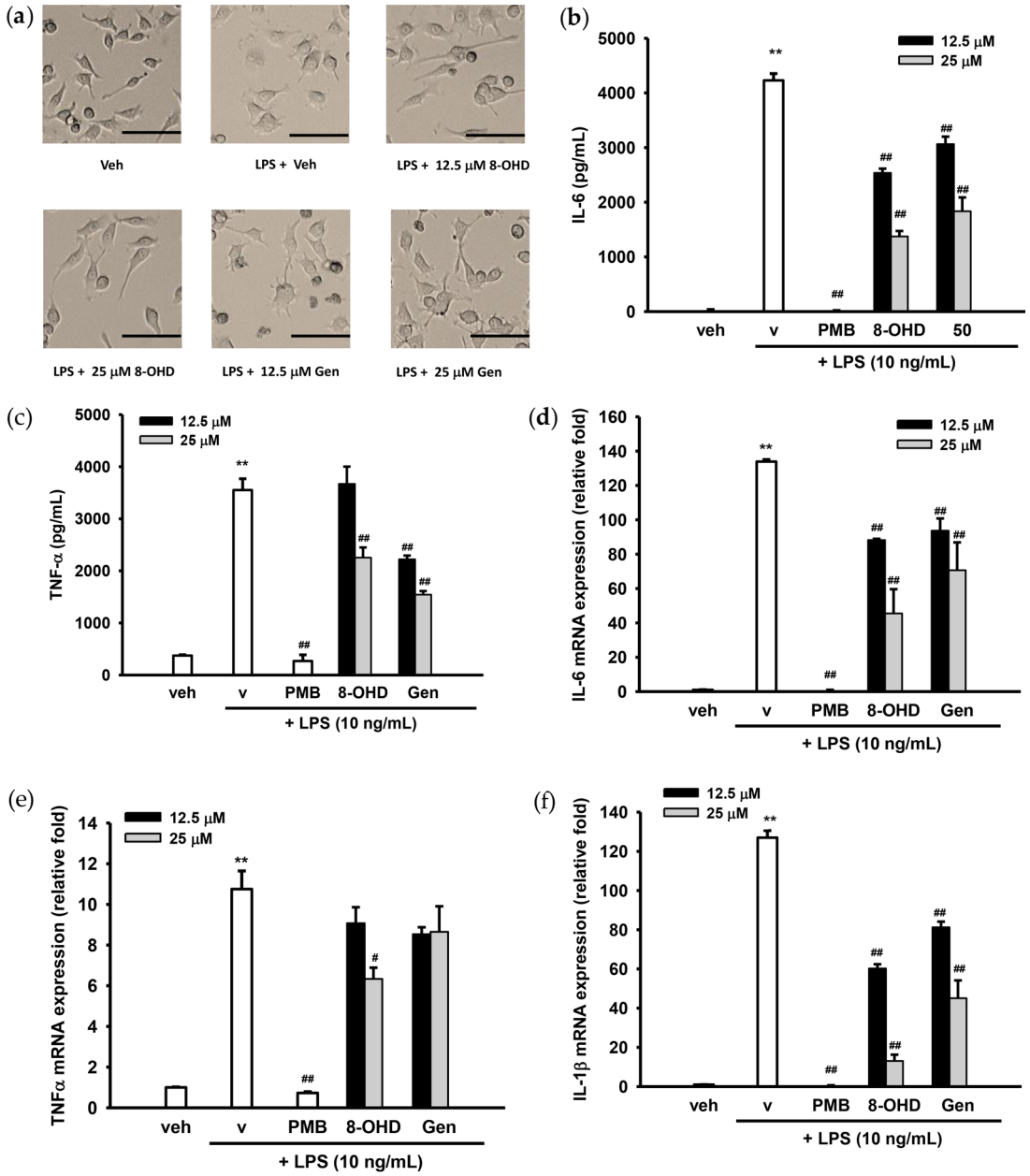

Figure 2. Effects of 8-hydroxydaidzein (8-OHD) and genistein (Gen) on BV2 activation and the production and mRNA expression of pro-inflammatory cytokines in LPS-treated BV2 cells. (a) Representative images of BV2 microglia treated with indicated reagent for 20 h. Images were acquired with Nikon Eclipse Ti-E inverted microscope (scale bar, 50 μm). (b and c) BV2 cells were pretreated with the indicated reagent for 30 min and then stimulated with LPS for 20 h. Supernatant was collected for IL-6 and TNF-α assay, as described in the Materials and Methods. (d–f) RNA was isolated 4 h after LPS challenge, and mRNA expression levels of IL-6, TNF-α, and IL-1β were measured by RT-Q-PCR, as described in the Materials and Methods. Data are represented as the mean ± SD (n = 3). Statistical differences are presented ** $p < 0.01$ compared with the vehicle control (without LPS) and # $p < 0.05$; ## $p < 0.01$ compared with the LPS-treated vehicle.

(Amersham ECL Prime Western Blotting Detection Reagents, GE Healthcare). Some blots were stripped with Restore Western Blot stripping solution (Thermo Fisher Scientific, Rockford, IL, USA) to remove previous primary and secondary antibodies. After washes and blocking, the blots were reprobed with another primary antibody. The intensity of the band was analyzed with ImageJ software (National Institutes of Health, Bethesda, MD, USA).

Cyclooxygenase (COX)-2 Inhibition Assay. Inhibitory activities of the 8-OHD and Gen against COX-2 enzyme were determined using a fluorometric COX-2 inhibitor screening kit following the kit protocol. To calculate the initial velocity of COX-2 activity (RFU/sec), the slope of the early linear range of the enzyme reaction progress plot was made using the observed RFU vs time. The relative activity (V_i/V_o) was determined as the ratio between the initial velocity in the presence (V_i) and absence (V_o) of the inhibitor. The IC_{50} values were calculated from the regression analysis of a relative activity vs concentration plot and denoted the concentration of the sample required to inhibit 50% of the enzyme activity.

The enzyme kinetics of 8-OHD was further determined using various concentrations of substrate (arachidonic acid) either in the absence or in the presence of selected concentrations of 8-OHD. The mode of inhibition was determined by the Lineweaver–Burk double-reciprocal plot analysis.

Intracellular ROS Analysis. BV2 cells were cultured in black 96-well plates (2×10^5/well) overnight. Cells were washed with PBS and then stained with 20 μM 2′,7′-dichlorodihydrofluorescein diacetate

DOI: 10.1021/acs.jafc.8b00437
J. Agric. Food Chem. 2018, 66, 5790–5801

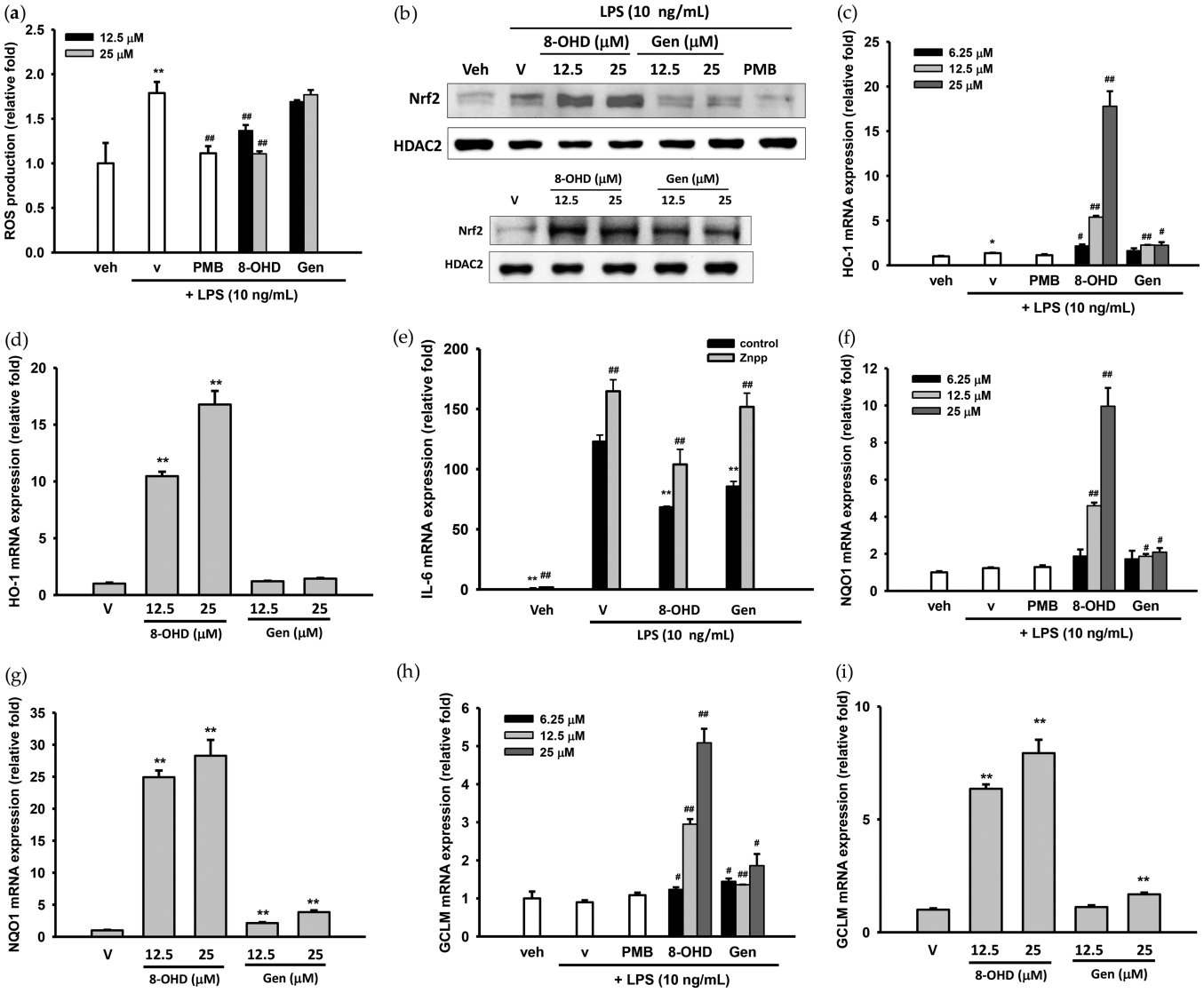

Figure 3. 8-Hydroxydaidzein (8-OHD) represses LPS-mediated ROS production and induces Nrf2 activation and target gene expression. (a) BV2 cells were pretreated with the indicated reagent for 30 min and then stimulated with LPS for 20 h. ROS production was measured as described in the Materials and Methods. Data are represented as the mean ± SD (n = 3). Statistical differences are presented ** $p < 0.01$ compared with the vehicle control (without LPS) and ## $p < 0.01$ compared with the LPS-treated vehicle. (b) BV2 cells were cultured with the indicated reagent for 4 h, and then nuclear extract was prepared. Protein levels of Nrf2 and HDAC2 (nuclear loading control) were detected by Western blotting. (c, f, h) BV2 cells were treated with indicated reagent for 30 min followed by LPS treatment for 4 h. RNA was prepared, and mRNA levels of HO-1, NQO1, and GCLM were determined by RT-Q-PCR. Data are represented as the mean ± SD (n = 3). Statistical differences are presented ** $p < 0.01$ compared with the vehicle control (without LPS) and ## $p < 0.01$ compared with the LPS-treated vehicle. (d, g, i) BV2 cells were cultured with indicated reagent for 6 h. RNA was prepared, and mRNA levels of HO-1, NQO1, and GCLM were determined by RT-Q-PCR. Data are represented as the mean ± SD (n = 3). Statistical differences are presented ** $p < 0.01$ compared with the vehicle control. (e) Effects of HO-1 inhibitor, Znpp, on the IL-6 expression. BV2 cells were pretreated for 30 min with Znpp (5 μM) followed by indicated treatment for 30 min before LPS (10 ng/mL) insult for 4 h. IL-6 expression was measured by RT-Q-PCR. Statistical differences are presented ** $p < 0.01$ compared with the LPS-treated vehicle and ## $p < 0.01$ compared with relative no inhibitor group.

(H_2DCFDA, Invitrogen), a fluorogenic dye that measures hydroxyl, peroxyl, and other reactive oxygen species (ROS) activity within the cell at 37 °C for 30 min in the dark and then washed with PBS. Cells were treated with indicated reagent for 30 min followed by LPS for 20 h. The signals were then read at EX485 nm/Em535 nm.

Statistical Analysis. Data were presented as means ± SD and analyzed by one-way analysis of variance (ANOVA) with Tukey's post hoc test. A p value of <0.05 was taken to be significant.

RESULTS

Effects of 8-Hydroxydaidzein (8-OHD) and Genistein (Gen) on Lipopolysaccharide (LPS)-Mediated Inducible Nitric Oxide Synthase (iNOS) Expression and Nitric Oxide (NO) Production.

The inhibitory effects of 8-OHD and structurally similar trihydroxyisoflavone Gen on neuroinflammation were investigated in LPS-stimulated mouse microglial cell line BV2. LPS (10 ng/mL) plus vehicle (0.1% DMSO) stimulated NO production from the basal level (1.5 ± 0.2 μM) to 39.2 ± 1.3 μM (Figure 1a) and concurrently caused 37% BV2 cell death after 20 h (Figure 1b). This supports the notion that LPS insult resulted in microglia death.[29] Pretreatment cells with LPS inhibitor polymyxin B (PMB) 30 min before LPS challenge completely blocked NO production and

DOI: 10.1021/acs.jafc.8b00437
J. Agric. Food Chem. 2018, 66, 5790−5801

cytotoxicity. Pretreatment cells with 12.5 and 25 μM 8-OHD dose dependently decreased LPS-stimulated NO production by 78% and 94% in conjunction with increased cell viability to 90% and 96% of vehicle control, respectively. In comparison, 12.5 and 25 μM Gen inhibited NO production by 52% and 78% and restored cell viability to 69% and 81% of vehicle control, respectively. These results indicate that 8-OHD inhibited LPS-mediated NO production and cytotoxicity more effectively than Gen did in BV2 microglia.

When 8-OHD and Gen was added 30 min after LPS challenge, NO inhibitory effects are substantial but less than pretreatment (Figure 1c). This demonstrates that these two isoflavones exert anti-NO effects at least in part via prevention of activation of cell signaling pathways. Significant anti-NO efficacies of 8-OHD and Gen were also observed in LPS-treated RAW264.7 murine macrophages, indicating they also exerted inhibitory effects in systematic inflammation (SFigure 3).

Nitric oxide (NO) is produced from L-arginine by iNOS in microglia in response to proinflammatory stimuli.[30] Figure 1d shows that treatment of BV2 cells with LPS (10 ng/mL) for 4 h significantly upregulated the iNOS transcript level by 33-fold and PMB (10 μg/mL) completely blocked its expression. 8-OHD (12.5 and 25 μM) dose dependently inhibited iNOS mRNA expression by 34% and 64%, respectively. On the other hand, only high concentration (25 μM) of Gen significantly decreased iNOS mRNA level by 25% ($p < 0.05$). Figure 1e shows that LPS (10 ng/mL) dramatically increased iNOS protein expression after 16 h treatment. 8-OHD and Gen markedly attenuated LPS-mediated iNOS expression in a dose-dependent manner. This result suggests that the inhibitory effects of 8-OHD and Gen on nitric oxide production were due to downregulation of iNOS expression in both transcription and translation stages.

8-OHD Alleviates LPS-Mediated BV2 Activation and Downregulates Expression of Pro-inflammatory Cytokines, Chemokines, and Interferon Regulatory Factors (IRFs). Conventional BV2 cells have ramified shapes with filopodia. They quickly convert to large, round, or amoeboid shapes once activated by LPS.[3] Figure 2a shows that BV2 cells treated with vehicle had the typical branching shape with smaller soma. BV2 cells treated with LPS (10 ng/mL) plus vehicle for 20 h showed the enlargement of the microglial cell body with retracted filopodia. In contrast, elongated filopodia and smaller soma were observed in those treated with LPS and 8-OHD as compared with LPS plus vehicle. These data show that 8-OHD restored the ramified state of BV2 cells and effectively alleviated BV2 activation. Gen, however, showed less inhibitory effect against BV2 activation.

Tumor necrosis factor (TNF)-α, interleukin (IL)-6, and IL-1β are the major pro-inflammatory cytokines elicited by LPS-activated macroglia.[31] LPS (10 ng/mL) treatment for 20 h markedly induced production of IL-6 and TNF-α, and cotreatment with PMB completely abolished their secretion (Figure 2b and 2c). Treatment cells with 8-OHD and Gen (12.5 and 25 μM) effectively repressed excessive production of IL-6 in a dose-dependent manner and was associated with downregulation of IL-6 mRNA expression (Figure 2d). 8-OHD inhibited IL-6 secretion and expression more potently than Gen ($p < 0.05$). However, 8-OHD decreased TNF-α secretion less powerfully than Gen ($p < 0.01$) (Figure 2c). The inhibitory effect of 8-OHD, but not Gen, on TNF-α production was related to the decreased mRNA expression (Figure 2e). 8-OHD and Gen (12.5 and 25 μM) showed marked inhibitory effects on LPS-mediated IL-1β mRNA expression in a dose-dependent manner, and 8-OHD was more effective than Gen (Figure 2f). These data indicate that 8-OHD inhibited the production of proinflammatory cytokines mainly through downregulation of mRNA expression.

There is considerable evidence that the β-chemokines CCL2 (CC chemokine ligand 2)/MCP-1 (monocyte chemoattractant protein-1) and CCL3 (CC chemokine ligand 3)/MIP1α (macrophage inflammatory protein-1α) play an important role in CNS inflammation.[32] A significant induction of CCL2/MCP-1 and CCL3/MIP1α transcription was observed 4 h after LPS (10 ng/mL) treatment, and PMB completely abolished the induction. 8-OHD inhibited their expression more significantly than Gen did (SFigures 4a and 4b).

The interferon-regulatory factor (IRF) family of transcription factors comprises nine members and is involved in LPS-mediated TLR (Toll-like receptor) signaling.[33] It has been shown that IRF1 is required for iNOS expression.[34] IRF-7 is the master regulator of type-I interferon-dependent immune responses.[35] We found that treatment of BV2 cells with LPS (10 ng/mL) for 4 h induced IRF1 and IRF7 expression and cotreatment with 25 μM 8-OHD and Gen attenuated IRF1 and IRF7 upregulation with similar effectiveness (SFigures 4c, 4d).

8-OHD Represses Reactive Oxygen Species (ROS) Production and Induces Nrf2 Activation. It has been reported that in response to LPS, microglia release ROS that cause neurotoxicity.[36] Treatment of cells with LPS (10 ng/mL) resulted in an increase in intracellular ROS generation. 8-OHD (12.5 and 25 μM) dose-dependently quenched intracellular ROS; on the other hand, Gen did not exert measurable ROS scavenging activity (Figure 3a).

It has been reported that isoflavones counteract oxidative stress in inflammatory diseases by modulating the redox-sensitive Nrf2 defense pathway.[15] We found that 8-OHD was more potent than Gen in inducing Nrf2 nuclear translocation regardless of the presence or absence of LPS in BV2 cells (Figure 3b).

Heme oxygenase 1 (HO-1), a Nrf2 target gene, is well known to have antioxidant and anti-inflammatory properties.[37] Figure 3c and 3d shows that 8-OHD induced more abundant HO-1 mRNA than Gen regardless of LPS stimulation. The effect on HO-1 protein upregulation was less pronounced than HO-1 mRNA expression (SFigure 5).

To ascertain HO-1 dependency of proinflammatory cytokine inhibition, we tested the consequence of chemical inhibition of HO-1. It was found that zinc protoporphyrin IX (ZnPP, 5 μM), a potent competitive inhibitor of HO enzyme activity, significantly enhanced IL-6 expression ($p < 0.01$) and reversed IL-6 inhibitory effects by 8-OHD and Gen ($p < 0.01$). This result supports the notion that HO-1 contributes to the resolution of inflammation (Figure 3e).

We further investigated how 8-OHD and Gen affected expression of other Nrf2-driven genes, NAD(P)H quinone dehydrogenase 1 (NQO1), and the modifier subunit of glutamate cysteine ligase (GCLM). 8-OHD treatment induced NQO1 and GCLM mRNA expression dose-dependently in the presence and absence of LPS (Figure 3f–i). In the absence of LPS, 8-OHD (25 μM) upregulated mRNA expression of NQO1 and GCLM by 28.2- and 7.9- fold, respectively. In comparison, 25 μM Gen only enhanced 3.8-fold NQO1 and 1.7-fold GCLM mRNA expression in the absence of LPS. These data indicate that 8-OHD activates Nrf2 signaling pathway much more strongly than Gen does. This agrees with

DOI: 10.1021/acs.jafc.8b00437
J. Agric. Food Chem. 2018, 66, 5790−5801

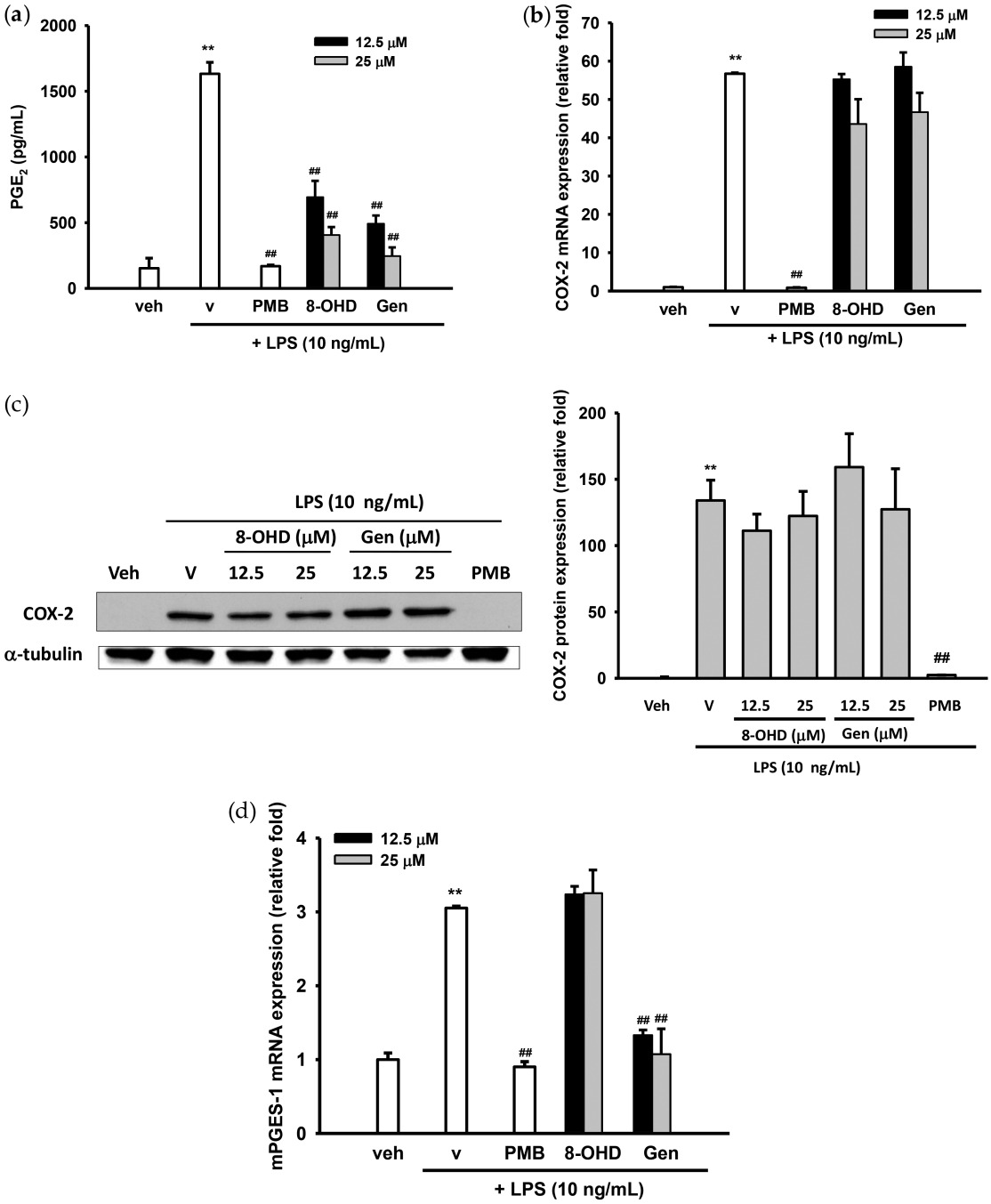

Figure 4. Effects of 8-hydroxydaidzein (8-OHD) and genistein (Gen) on PGE_2 production and expression of COX-2 and mPGES-1 in LPS-treated BV2 cells. (a) BV2 cells were pretreated for 0.5 h with vehicle (0.1% DMSO), polymyxin B (PMB, 10 μg/mL), or the indicated concentration of compound and then stimulated with LPS (10 ng/mL) for 20 h. Supernatant was collected for PGE_2 measurement, as described in the Materials and Methods. (b and d) BV2 cells were pretreated with the indicated reagent for 30 min and then stimulated with LPS for 4 h. RNA was isolated, and mRNA levels of COX-2 and mPGES-1 were measured by RT-Q-PCR, as described in the Materials and Methods. (c) Total protein was prepared 16 h after LPS challenge. Protein levels of COX-2 and α-tubulin were detected by Western blotting, as described in the Materials and Methods. Representative blots from one of the three independent experiments are shown. Band intensities were quantified by ImageJ software and indicated as relative folds of COX-2/α-tubulin. Data are represented as the mean ± SD (n = 3). Statistical differences are presented ** $p < 0.01$ compared with the vehicle control (without LPS) and ## $p < 0.01$ compared with the LPS-treated vehicle (0.1% DMSO).

the notion that *ortho*-diphenol, but not *meta*-diphenol, serves as a potent Nrf2 activator.[9]

Effects of 8-OHD and Gen on Prostaglandin E_2 (PGE_2) Production and Expression of Cyclooxygenase (COX)-2 and Microsomal Prostaglandin E2 Synthase-1 (mPGES-1). It was found that BV2 cells produced PGE_2 in response to LPS (10 ng/mL) stimulation. 8-OHD and Gen (12.5 and 25 μM) dose-dependently inhibited LPS-mediated PGE_2 production, and Gen was slightly more potent (Figure 4a).

PGE_2 is generated from arachidonic acid by the sequential enzymatic action of COX and PGES during inflammation.[38] There are two forms of COX, a constitutively expressed COX-1 and an inducible COX-2. LPS strongly stimulated COX-2 mRNA, and protein expression and PMB (10 μg/mL)

DOI: 10.1021/acs.jafc.8b00437
J. Agric. Food Chem. 2018, 66, 5790−5801

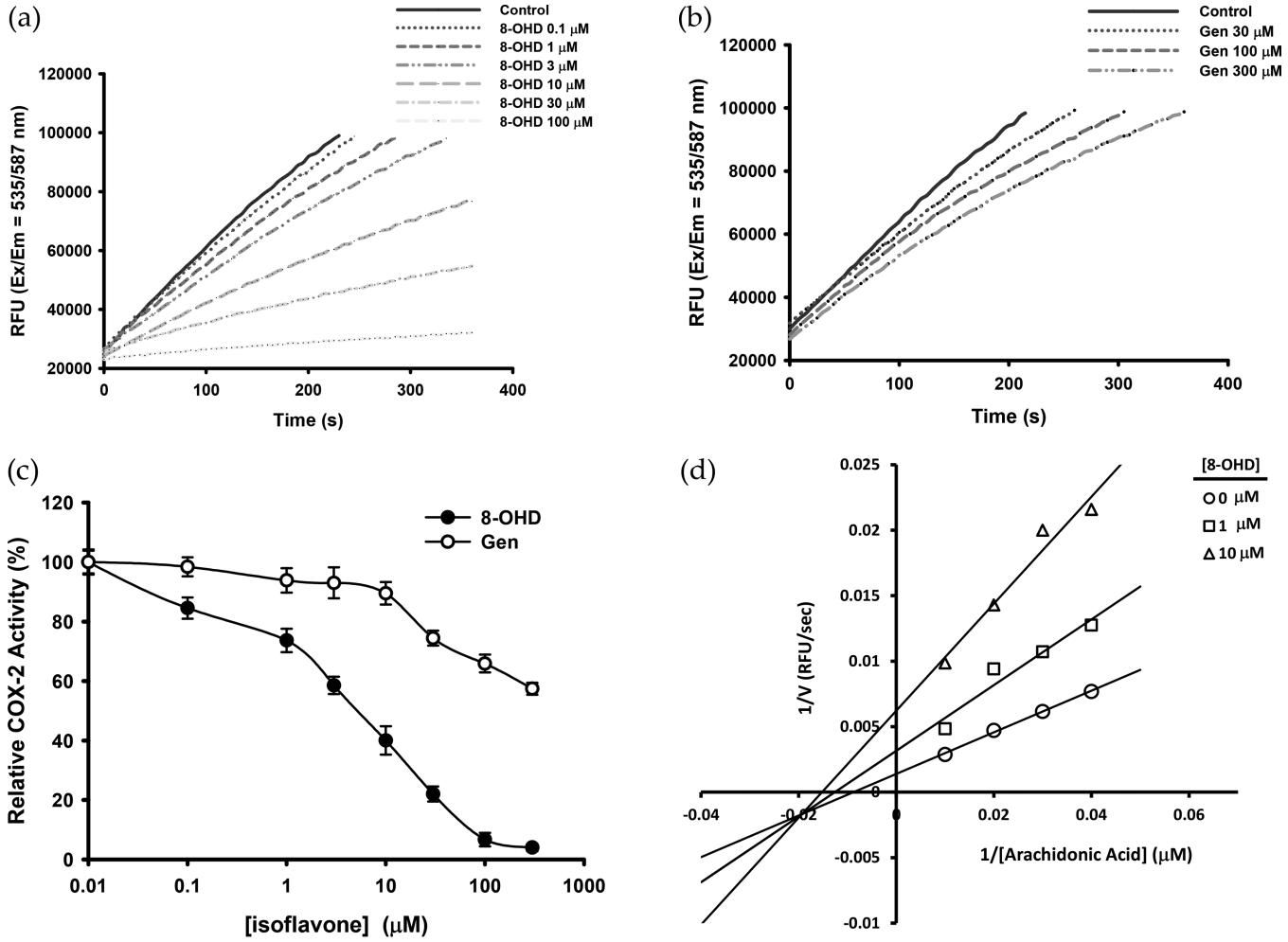

Figure 5. Effects of 8-hydroxydaidzein (8-OHD) and genistein (Gen) on COX-2 enzyme activity in vitro. (a and b) Progress curves for the inhibition of COX-2 by 8-OHD and Gen. COX-2 activity was analyzed as described in the Materials and Methods. (c) Inhibition of COX-2 activity with 8-OHD and Gen. (d) Lineweaver–Burk double reciprocal plot of the rate of prostaglandin G_2 formation (v) versus substrate concentration (arachidonic acid) in the absence and presence of 8-OHD.

completely blocked their expression. However, neither 8-OHD nor Gen significantly attenuated their expression (Figure 4b and 4c).

Three forms of PGESs regulate the final step in the synthesis of PGE_2. Among them, mPGES-1 is an inducible form. Consequently, we determined if downregulation of mPGES-1 transcription contributed to the inhibitory effects of 8-OHD and Gen on PGE_2 production in LPS-activated BV2 cells. The result shows that only Gen, but not 8-OHD (12.5 and 25 μM), reduced mPGES-1 mRNA expression (Figure 4d). These results indicate that Gen blocked LPS-mediated PGE_2 production in BV2 cells through suppressing mPGES-1 transcription rather than by inhibiting COX-2 expression.

8-OHD Inhibits Cyclooxygenase (COX)-2 Enzyme Activity. Lots of NSAIDs (nonsteroidal anti-inflammatory drugs) block PGE_2 synthesis via inhibiting COX enzyme activity. To investigate whether 8-OHD and Gen inhibit COX-2 enzyme activities, a commercial COX-2 assay kit that is based on the fluorometric detection of prostaglandin G_2, the intermediate product generated by the COX enzyme, was used. The COX-2 inhibition assay was carried out using serial dilutions of 8-OHD and Gen. 8-OHD (0.1–100 μM) was found to inhibit COX-2 activity in a dose-dependent manner, with an IC_{50} of 8.9 ± 1.2 μM (Figures 5a and 5c). As a comparison, higher concentrations of Gen (30–300 μM) were needed to exert a significant COX-2 inhibitory effect, with an IC_{50} of >1 mM (Figure 5b and 5c).

To understand the mode of COX-2 inhibition by 8-OHD, we conducted an enzyme kinetics analysis of the COX-2 activity in the presence of various concentrations of 8-OHD and the substrate arachidonic acid. The Lineweaver–Burk plot analysis reveals 8-OHD exhibited a mixed-type inhibition, with an intersect below the x axis. This mixed type system occurs when the inhibitor (8-OHD) is capable of binding to both the free enzyme (COX-2) and the enzyme–substrate (COX-2-arachidonic acid) complex. The position of the intersection indicates that the effect of 8-OHD is to lower the apparent value of V_{max} and to decrease the apparent value of K_m. Therefore, 8-OHD is capable of preventing catalysis regardless of whether arachidonic acid is bound to the COX-2. These results demonstrate for the first time that 8-OHD reduced PGE_2 production by inhibiting COX-2 enzyme activity rather than by down-regulating COX-2 expression.

8-OHD Inhibits Phosphorylation of Akt and p65 NF-κB. It is well known that LPS activates TLR and leads to PI3K activation. TLR-mediated Akt phosphorylation in turn increases the transcription activity of the p65 subunit of NF-κB.[39] Therefore, to assess whether 8-OHD and Gen influence PI3K/

DOI: 10.1021/acs.jafc.8b00437
J. Agric. Food Chem. 2018, 66, 5790–5801

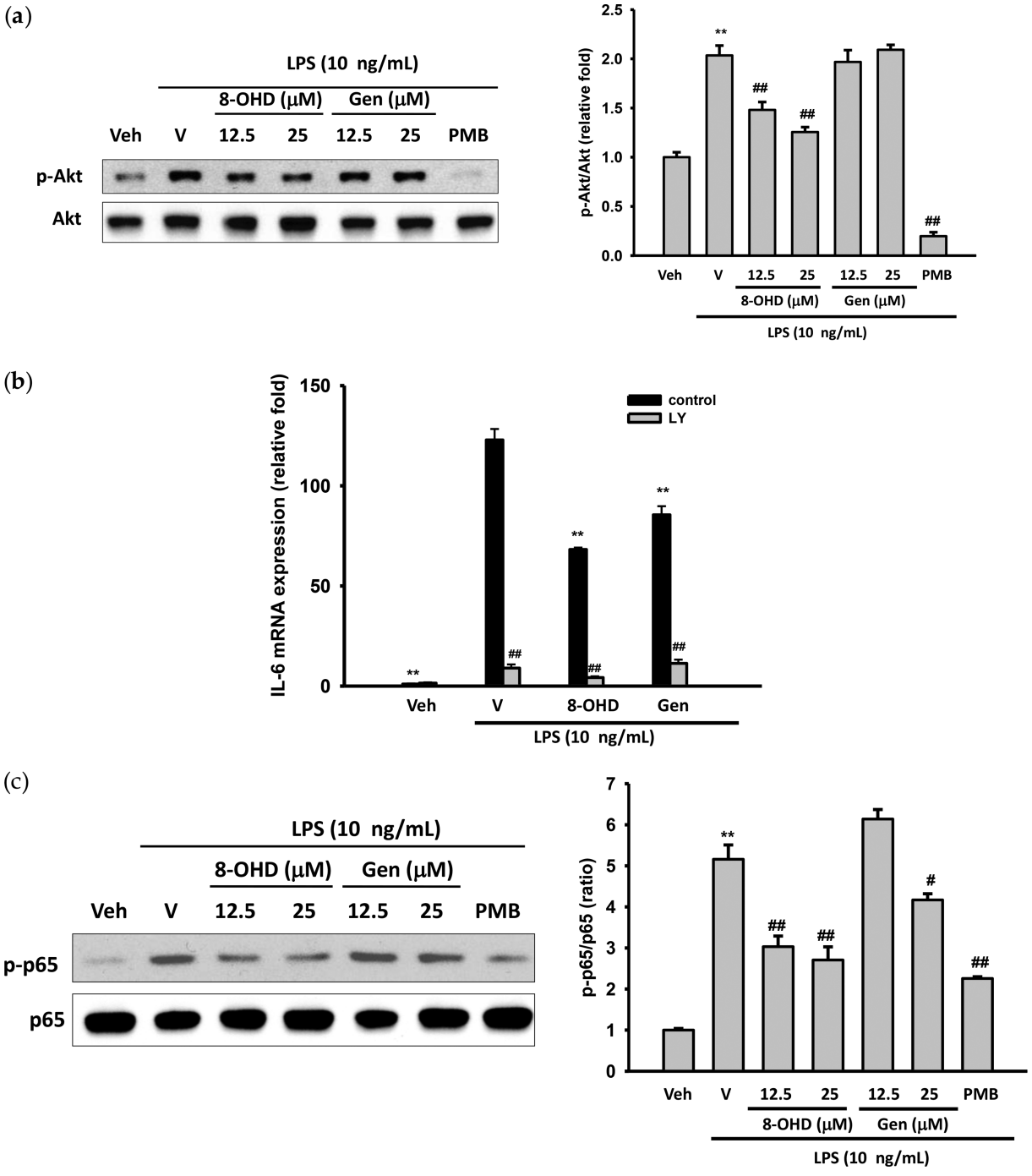

Figure 6. Effects of 8-hydroxydaidzein (8-OHD) and genistein (Gen) on LPS-mediated activation of Akt and NF-κB in BV2 cells. (a, c) BV2 cells were pretreated with the indicated reagent for 30 min and then stimulated for 30 min with LPS (10 ng/mL). Western blots were performed using the appropriate antibodies. Representative blots from three independent experiments are shown. Densitometry is presented as the mean ± SD of three independent experiments. Statistical differences are presented ** $p < 0.01$ compared with the vehicle control (without LPS) and # $p < 0.05$; ## $p < 0.01$ compared with the LPS-treated vehicle. (b) Effects of PI3K/Akt inhibitor, LY294002, on the IL-6 expression. BV2 cells were pretreated for 30 min with LY294002 (25 μM) followed by vehicle (0.1% DMSO), 8-OHD (25 μM), or Gen (25 μM) for 30 min before LPS (10 ng/mL) insult for 4 h. IL-6 expression was measured by RT-Q-PCR.

Akt phosphorylation, Western blot analysis was performed in BV2 cells 30 min after treatment with LPS. Figure 6a shows that LPS induced phosphorylation of Akt at Ser^{473}, and only 8-OHD, but not Gen, significantly inhibited Akt activation.

To investigate the functional effect of Akt activation, IL-6 mRNA expression in the presence of the PI3K/Akt inhibitor LY294002 was measured. It was found that LY294002 (25 μM) treatment strongly decreased the expression levels of LPS-induced IL-6 mRNA (Figure 6b), indicating that Akt activation is involved in LPS-induced IL-6 expression. Furthermore, additive inhibitory effects were noted for those treated with the combination of LY294002 and 8-OHD but not for those with the combination of LY294002 and Gen. Similar results were also observed for IL-1β mRNA expression (SFigure 6). In conclusion, these results indicate that inhibition of the PI3K/

DOI: 10.1021/acs.jafc.8b00437
J. Agric. Food Chem. 2018, 66, 5790−5801

Akt signaling pathway is associated with the anti-inflammatory activity of 8-OHD.

NF-κB, a transcription factor activated by LPS, controls the expression of pro-inflammatory enzymes and cytokines. To further investigate the effects of 8-OHD and Gen on NF-κB activation, we used Western blot to examine the cellular level of phosphorylated NF-κB p65. We found that LPS treatment for 30 min strongly stimulated p-p65 at Ser^{536}, and 8-OHD (12.5 and 25 μM) and Gen (25 μM) significantly inhibited its activation (Figure 6c). Taken together, these results show that 8-OHD treatment reduces LPS-induced inflammatory responses in BV2 cells partially through inhibiting Akt and NF-κB activation.

DISCUSSION

Soybean is one of the earliest so-called functional foods, as it contains various types of isoflavones and offers health benefits independent of its nutrient content.[14] Isoflavones are absorbed minutes after intake due to their small molecular weights and favorable lipophilic property.[40] Isoflavones then go through diverse and extensive metabolism, including oxidation, reduction, and conjugation, and this is one of the major reasons contributing to their low oral bioavailability.[41] The major metabolites identified in human plasma are phase II metabolites, primarily as glucuronides and sulfates, but not phase I oxidative metabolites.[42] Pharmacokinetic studies reveal the maximum concentration of total isoflavones can reach several micromolar, while aglycones only account for hundreds of nanomolar.[43−45]

Increasing evidence has highlighted the potential of isoflavones to prevent chronic diseases in which inflammation plays a key role.[46] It is widely accepted that microglial activation and inflammation contributes to neurodegenerative diseases.[47] In this report, we analyzed the response of aglycones (8-OHD and Gen) up to 25 μM in LPS-activated BV2 microglia. Such concentrations are widely used in vitro, although systemic bioavailability of isoflavones is much lower.

Excess production of NO by iNOS in microglia has been shown to be toxic to neurons.[48] We have demonstrated that 8-OHD prevents NO production by inhibiting expression of iNOS mRNA and protein and mitigates cytotoxicity. The morphology of BV2 microglia cells along with data on the expression and synthesis of iNOS indicate that 8-OHD suppresses pro-inflammation-induced microglial activation. However, Gen, a well-known anti-inflammatory isoflavone with *meta*-diphenol structure, shows a weaker inhibitory efficacy than 8-OHD on LPS-mediated iNOS expression, activation, and cytotoxicity in BV2 cells.

TNF-α, IL-6, and IL-1β are the initiators of the inflammatory response. Chemokines, such as CCL2 and CCL3, are crucial in the regulation of proliferation and migration of microglia to inflammation sites. Interferon-regulatory factor (IRF) families are positive regulators of the inflammatory genes in microglia. In this research, we found that 8-OHD inhibited LPS-mediated mRNA expression of TNF-α, IL-6, IL-1β, CCL2, CCL3, IRF1, and IRF7 in dose-dependent manners. In comparison, similar or slightly less inhibitory effects of Gen on pro-inflammatory gene expression were found.

Nrf2 is the major regulator of cytoprotective gene expression, and its activation is critical in modulating redox homeostasis and regulating inflammatory conditions.[49] Here we found that 8-OHD activated Nrf2 and in turn induced HO-1, NQO1, and GCLM expression much stronger than Gen did. Blockade of HO-1 activity with ZnPP-IX partly reversed their anti-inflammatory effects. Furthermore, 8-OHD, rather than Gen, quenched LPS-stimulated intracellular ROS generation. It is now understood that electrophilic Michael acceptors are Nrf2 activators,[9] and *ortho*-hydroquinones and *para*-hydroquinones, but not *meta*-hydroquinones, induce ARE-driven gene expression.[50] Our data support that 8-OHD with an *ortho*-diphenol electrophilic core is an effective Nrf2 activator and ROS scavenger. The anti-inflammatory activity of 8-OHD may be in great part attributed to activation of Nrf2, which inhibits transcriptional upregulation of proinflammatory cytokine genes and induces expression of Phase II enzymes.

COX-2 and mPGES-1 are both regulated at transcriptional levels, and both enzymes are important in the synthesis of PGE_2 during inflammation. We found that although LPS-induced PGE_2 was attenuated by 8-OHD and Gen, LPS-stimulated COX-2 mRNA or protein expression was not altered. Gen, but not 8-OHD, reduced PGE_2 production by downregulating LPS-mediated $mPGE_2$ transcription in BV2 cells.

In vitro enzyme activity inhibition assay found that Gen has an IC_{50} value for COX-2 more than 100-fold higher than that observed with 8-OHD. It has been reported that homodimeric COX enzymes function as heterodimers, with one subunit acting as a catalytic site and the second subunit acting as an allosteric site.[51] 8-OHD displayed mixed-type inhibition of COX-2 with respect to arachidonic acid as substrate, indicating 8-OHD binds to an allosteric site. The Lineweaver−Burk double-reciprocal plot intersected below the *x* axis, suggesting that COX-2−8-OHD complex has an increased affinity for arachidonic acid but that the COX-2-arachidonic acid-8-OHD complex forms product prostaglandin G_2 more slowly than the COX-2-arachidonic acid complex. These observations suggest that 8-OHD inhibited LPS-mediated PGE_2 production through inhibition of COX-2 enzyme activity.

ROS are critical for activation of Akt and NF-κB in LPS/TLR4 signaling in microgia.[52] We found that LPS strongly induced Akt phosphorylation, which was severely compromised by 8-OHD but not Gen. Addition of PI3K inhibitor augmented the antiproinflammatory cytokine activity of 8-OHD rather than that of Gen. The phosphorylation of p65 at Ser^{536} is important for NF-κB activation and nuclear translocation.[53] The classical NF-κB pathway mediates microglial activation and neuron death.[54] In this report, we found that 8-OHD strongly inhibited LPS-induced p65 NF-κB phosphorylation in BV2 cells. These results highlight how 8-OHD regulates the anti-inflammatory response by controlling Akt and NF-κB signaling pathways.

Current results also demonstrate a good correlation between Nrf2 activation, ROS scavenging, and inactivation of Akt and NF-κB in 8-OHD-treated BV2 cells. There are complex molecular cross-talks between Nrf2 and NF-κB pathways in order to maintain redox homeostasis.[6] It has recently been reported that in addition to upregulating expression of antioxidant genes, Nrf2 also serves as a direct negative regulator for proinflammatory cytokine expression.[55] Our study strongly indicates that 8-OHD-stimulated Nrf2 signaling appears to suppress LPS-induced activation of Akt and NF-κB signaling.

In conclusion, our data indicate that 8-OHD inhibits production of NO, TNF-α, and IL-6 as well as attenuates expression of genes encoding iNOS, pro-inflammatory cytokines, chemokines, and IRFs in LPS-activated BV-2 microglia. The downregulation of proinflammatory gene

DOI: 10.1021/acs.jafc.8b00437
J. Agric. Food Chem. 2018, 66, 5790−5801

expression is in great part attributed to the activation of the Keap1-Nrf2-ARE pathway, which upregulates the expression of Phase II antioxidant enzymes, HO-1, NQO-1, and GCLM, and confers resistance to LPS-mediated oxidative stress. 8-OHD also mitigates phosphorylation of Akt and NF-κB, which induce proinflammatory gene expression. In addition, 8-OHD inhibited PGE_2 production mainly through mixed-type inhibition of COX-2 enzyme activity.

■ ASSOCIATED CONTENT

Supporting Information

The Supporting Information is available free of charge on the ACS Publications website at DOI: 10.1021/acs.jafc.8b00437.

Supplemental Materials and methods; primer pairs used in RT-Q-PCR; primary antibodies used in Western blotting; chemical structures of Genistein and 8-hydroxydaidzein; ultraperformance liquid chromatography (UPLC) profile of isolated 8-OHD; treatment of 8-OHD and Gen inhibited LPS-mediated NO production in RAW264.7 cells; effects of 8-hydroxydaidzein (8-OHD) and genistein (Gen) on the expression of chemokines and interferon-regulatory factors (IRFs) in LPS-treated BV2 cells; 8-OHD induced HO-1 protein expression in the presence and absence of LPS in BV2 cells; effects of PI3K/Akt inhibitor, LY294002, on the IL-1β expression; additional references (PDF)

■ AUTHOR INFORMATION

Corresponding Author

*E-mail: imwu@mail.cnu.edu.tw. Tel.: +886-6-266-4911 ext 2520. Fax: +886-6- 266-2135.

ORCID

Jui-Hung Yen: 0000-0003-2551-350X

Ming-Jiuan Wu: 0000-0003-3327-828X

Author Contributions

§P.-S.W. and H.-Y.D.: These authors contributed equally to this work.

Funding

This research was supported by research grants NSC102-2320-B-041-003-MY3 and MOST 106-2320-B-041-006-MY3 from the Ministry of Science and Technology, Taipei, Taiwan.

Notes

The authors declare no competing financial interest.

■ REFERENCES

(1) Brown, G. C.; Neher, J. J. Microglial phagocytosis of live neurons. *Nat. Rev. Neurosci.* **2014**, *15*, 209−216.

(2) Michell-Robinson, M. A.; Touil, H.; Healy, L. M.; Owen, D. R.; Durafourt, B. A.; Bar-Or, A.; Antel, J. P.; Moore, C. S. Roles of microglia in brain development, tissue maintenance and repair. *Brain* **2015**, *138*, 1138−59.

(3) Kettenmann, H.; Hanisch, U. K.; Noda, M.; Verkhratsky, A. Physiology of microglia. *Physiol. Rev.* **2011**, *91*, 461−553.

(4) Mizuno, T. Neuron−microglia interactions in neuroinflammation. *Clin. Exp. Neuroimmunol.* **2015**, *6*, 225−231.

(5) Thameem Dheen, S.; Kaur, C.; Ling, E. A. Microglial activation and its implications in the brain diseases. *Curr. Med. Chem.* **2007**, *14*, 1189−1197.

(6) Wardyn, J. D.; Ponsford, A. H.; Sanderson, C. M. Dissecting molecular cross-talk between Nrf2 and NF-kappaB response pathways. *Biochem. Soc. Trans.* **2015**, *43*, 621−6.

(7) Hayes, J. D.; Dinkova-Kostova, A. T. The Nrf2 regulatory network provides an interface between redox and intermediary metabolism. *Trends Biochem. Sci.* **2014**, *39*, 199−218.

(8) Zhang, H.; Tsao, R. Dietary polyphenols, oxidative stress and antioxidant and anti-inflammatory effects. *Current Opinion in Food Science* **2016**, *8*, 33−42.

(9) Magesh, S.; Chen, Y.; Hu, L. Small molecule modulators of Keap1-Nrf2-ARE pathway as potential preventive and therapeutic agents. *Med. Res. Rev.* **2012**, *32*, 687−726.

(10) Natoli, G.; De Santa, F. Shaping alternative NF-kappaB-dependent gene expression programs: new clues to specificity. *Cell Death Differ.* **2006**, *13*, 693−6.

(11) Sakurai, H.; Chiba, H.; Miyoshi, H.; Sugita, T.; Toriumi, W. IkappaB kinases phosphorylate NF-kappaB p65 subunit on serine 536 in the transactivation domain. *J. Biol. Chem.* **1999**, *274*, 30353−6.

(12) Saponaro, C.; Cianciulli, A.; Calvello, R.; Dragone, T.; Iacobazzi, F.; Panaro, M. A. The PI3K/Akt pathway is required for LPS activation of microglial cells. *Immunopharmacol. Immunotoxicol.* **2012**, *34*, 858−65.

(13) Tsao, R. Chemistry and biochemistry of dietary polyphenols. *Nutrients* **2010**, *2*, 1231−46.

(14) Wang, Q.; Ge, X.; Tian, X.; Zhang, Y.; Zhang, J.; Zhang, P. Soy isoflavone: The multipurpose phytochemical (Review). *Biomed. Rep.* **2013**, *1*, 697−701.

(15) Mann, G. E.; Bonacasa, B.; Ishii, T.; Siow, R. C. Targeting the redox sensitive Nrf2-Keap1 defense pathway in cardiovascular disease: protection afforded by dietary isoflavones. *Curr. Opin. Pharmacol.* **2009**, *9*, 139−45.

(16) Moskot, M.; Montefusco, S.; Jakobkiewicz-Banecka, J.; Mozolewski, P.; Wegrzyn, A.; Di Bernardo, D.; Wegrzyn, G.; Medina, D. L.; Ballabio, A.; Gabig-Ciminska, M. The phytoestrogen genistein modulates lysosomal metabolism and transcription factor EB (TFEB) activation. *J. Biol. Chem.* **2014**, *289*, 17054−69.

(17) Jeong, J. W.; Lee, H. H.; Han, M. H.; Kim, G. Y.; Kim, W. J.; Choi, Y. H. Anti-inflammatory effects of genistein via suppression of the toll-like receptor 4-mediated signaling pathway in lipopolysaccharide-stimulated BV2 microglia. *Chem.-Biol. Interact.* **2014**, *212*, 30−9.

(18) Lee, Y. W.; Lee, W. H. Protective effects of genistein on proinflammatory pathways in human brain microvascular endothelial cells. *J. Nutr. Biochem.* **2008**, *19*, 819−25.

(19) Mirahmadi, S. M.; Shahmohammadi, A.; Rousta, A. M.; Azadi, M. R.; Fahanik-Babaei, J.; Baluchnejadmojarad, T.; Roghani, M. Soy isoflavone genistein attenuates lipopolysaccharide-induced cognitive impairments in the rat via exerting anti-oxidative and anti-inflammatory effects. *Cytokine+* **2018**, *104*, 151−159.

(20) Xiao, B. X.; Feng, L.; Cao, F. R.; Pan, R. L.; Liao, Y. H.; Liu, X. M.; Chang, Q. Pharmacokinetic profiles of the five isoflavonoids from Pueraria lobata roots in the CSF and plasma of rats. *J. Ethnopharmacol.* **2016**, *184*, 22−9.

(21) Liu, M. H.; Lin, Y. S.; Sheu, S. Y.; Sun, J. S. Anti-inflammatory effects of daidzein on primary astroglial cell culture. *Nutr. Neurosci.* **2009**, *12*, 123−34.

(22) Chang, T. S. Isolation, bioactivity, and production of ortho-hydroxydaidzein and ortho-hydroxygenistein. *Int. J. Mol. Sci.* **2014**, *15*, 5699−716.

(23) Esaki, H.; Onozaki, H.; Morimitsu, Y.; Kawakishi, S.; Osawa, T. Potent Antioxidative Isoflavones Isolated from Soybeans Fermented with Aspergillus saitoi. *Biosci., Biotechnol., Biochem.* **1998**, *62*, 740−6.

(24) Fujita, T.; Funako, T.; Hayashi, H. 8-Hydroxydaidzein, an aldose reductase inhibitor from okara fermented with Aspergillus sp. HK-388. *Biosci., Biotechnol., Biochem.* **2004**, *68*, 1588−90.

(25) Park, J. S.; Park, H. Y.; Kim, D. H.; Kim, D. H.; Kim, H. K. ortho-dihydroxyisoflavone derivatives from aged Doenjang (Korean fermented soypaste) and its radical scavenging activity. *Bioorg. Med. Chem. Lett.* **2008**, *18*, 5006−9.

(26) Chang, T. S.; Ding, H. Y.; Tai, S. S.; Wu, C. Y. Metabolism of the soy isoflavones daidzein and genistein by fungi used in the preparation of various fermented soybean foods. *Biosci., Biotechnol., Biochem.* **2007**, *71*, 1330−3.

DOI: 10.1021/acs.jafc.8b00437
J. Agric. Food Chem. 2018, 66, 5790−5801

(27) Chiang, C. M.; Ding, H. Y.; Tsai, Y. T.; Chang, T. S. Production of Two Novel Methoxy-Isoflavones from Biotransformation of 8-Hydroxydaidzein by Recombinant Escherichia coli Expressing O-Methyltransferase SpOMT2884 from Streptomyces peucetius. *Int. J. Mol. Sci.* **2015**, *16*, 27816−23.
(28) Carmichael, J.; DeGraff, W. G.; Gazdar, A. F.; Minna, J. D.; Mitchell, J. B. Evaluation of a tetrazolium-based semiautomated colorimetric assay: assessment of chemosensitivity testing. *Cancer Res.* **1987**, *47*, 936−942.
(29) Liu, B.; Wang, K.; Gao, H. M.; Mandavilli, B.; Wang, J. Y.; Hong, J. S. Molecular consequences of activated microglia in the brain: overactivation induces apoptosis. *J. Neurochem.* **2001**, *77*, 182−189.
(30) Saha, R. N.; Pahan, K. Regulation of inducible nitric oxide synthase gene in glial cells. *Antioxid. Redox Signaling* **2006**, *8*, 929−47.
(31) Wang, W. Y.; Tan, M. S.; Yu, J. T.; Tan, L. Role of pro-inflammatory cytokines released from microglia in Alzheimer's disease. *Ann. Transl. Med.* **2015**, *3*, 136.
(32) Chui, R.; Dorovini-Zis, K. Regulation of CCL2 and CCL3 expression in human brain endothelial cells by cytokines and lipopolysaccharide. *J. Neuroinflammation* **2010**, *7*, 1.
(33) Honda, K.; Taniguchi, T. IRFs: master regulators of signalling by Toll-like receptors and cytosolic pattern-recognition receptors. *Nat. Rev. Immunol.* **2006**, *6*, 644−658.
(34) Kamijo, R.; Harada, H.; Matsuyama, T.; Bosland, M.; Gerecitano, J.; Shapiro, D.; Le, J.; Koh, S. I.; Kimura, T.; Green, S. J.; et al. Requirement for transcription factor IRF-1 in NO synthase induction in macrophages. *Science* **1994**, *263*, 1612−5.
(35) Honda, K.; Yanai, H.; Negishi, H.; Asagiri, M.; Sato, M.; Mizutani, T.; Shimada, N.; Ohba, Y.; Takaoka, A.; Yoshida, N.; Taniguchi, T. IRF-7 is the master regulator of type-I interferon-dependent immune responses. *Nature* **2005**, *434*, 772−7.
(36) Block, M. L.; Zecca, L.; Hong, J. S. Microglia-mediated neurotoxicity: uncovering the molecular mechanisms. *Nat. Rev. Neurosci.* **2007**, *8*, 57−69.
(37) Wu, M. L.; Ho, Y. C.; Lin, C. Y.; Yet, S. F. Heme oxygenase-1 in inflammation and cardiovascular disease. *Am. J. Cardiovasc. Dis.* **2011**, *1*, 150−158.
(38) Williams, C. S.; Mann, M.; DuBois, R. N. The role of cyclooxygenases in inflammation, cancer, and development. *Oncogene* **1999**, *18*, 7908−16.
(39) Arbibe, L.; Mira, J.-P.; Teusch, N.; Kline, L.; Guha, M.; Mackman, N.; Godowski, P. J.; Ulevitch, R. J.; Knaus, U. G. Toll-like receptor 2-mediated NF-[kappa]B activation requires a Rac1-dependent pathway. *Nat. Immunol.* **2000**, *1*, 533−540.
(40) Franke, A. A.; Lai, J. F.; Halm, B. M. Absorption, distribution, metabolism, and excretion of isoflavonoids after soy intake. *Arch. Biochem. Biophys.* **2014**, *559*, 24−8.
(41) Yang, Z.; Kulkarni, K.; Zhu, W.; Hu, M. Bioavailability and pharmacokinetics of genistein: mechanistic studies on its ADME. *Anti-Cancer Agents Med. Chem.* **2012**, *12*, 1264−80.
(42) Hosoda, K.; Furuta, T.; Ishii, K. Metabolism and disposition of isoflavone conjugated metabolites in humans after ingestion of kinako. *Drug Metab. Dispos.* **2011**, *39*, 1762−7.
(43) Arai, Y.; Uehara, M.; Sato, Y.; Kimira, M.; Eboshida, A.; Adlercreutz, H.; Watanabe, S. Comparison of isoflavones among dietary intake, plasma concentration and urinary excretion for accurate estimation of phytoestrogen intake. *J. Epidemiol.* **2000**, *10*, 127−35.
(44) King, R. A.; Bursill, D. B. Plasma and urinary kinetics of the isoflavones daidzein and genistein after a single soy meal in humans. *Am. J. Clin. Nutr.* **1998**, *67*, 867−72.
(45) Takimoto, C. H.; Glover, K.; Huang, X.; Hayes, S. A.; Gallot, L.; Quinn, M.; Jovanovic, B. D.; Shapiro, A.; Hernandez, L.; Goetz, A.; Llorens, V.; Lieberman, R.; Crowell, J. A.; Poisson, B. A.; Bergan, R. C. Phase I pharmacokinetic and pharmacodynamic analysis of unconjugated soy isoflavones administered to individuals with cancer. *Cancer Epidemiol., Biomarkers Prev.* **2003**, *12*, 1213−1221.
(46) Yu, J.; Bi, X.; Yu, B.; Chen, D. Isoflavones: Anti-Inflammatory Benefit and Possible Caveats. *Nutrients* **2016**, *8*, 361.
(47) Liu, B.; Hong, J. S. Role of microglia in inflammation-mediated neurodegenerative diseases: mechanisms and strategies for therapeutic intervention. *J. Pharmacol. Exp. Ther.* **2003**, *304*, 1−7.
(48) Gresa-Arribas, N.; Vieitez, C.; Dentesano, G.; Serratosa, J.; Saura, J.; Sola, C. Modelling neuroinflammation in vitro: a tool to test the potential neuroprotective effect of anti-inflammatory agents. *PLoS One* **2012**, *7*, e45227.
(49) Kobayashi, M.; Yamamoto, M. Nrf2-Keap1 regulation of cellular defense mechanisms against electrophiles and reactive oxygen species. *Adv. Enzyme Regul.* **2006**, *46*, 113−40.
(50) Satoh, T.; McKercher, S. R.; Lipton, S. A. Nrf2/ARE-mediated antioxidant actions of pro-electrophilic drugs. *Free Radical Biol. Med.* **2013**, *65*, 645−57.
(51) Mitchener, M. M.; Hermanson, D. J.; Shockley, E. M.; Brown, H. A.; Lindsley, C. W.; Reese, J.; Rouzer, C. A.; Lopez, C. F.; Marnett, L. J. Competition and allostery govern substrate selectivity of cyclooxygenase-2. *Proc. Natl. Acad. Sci. U. S. A.* **2015**, *112*, 12366.
(52) Hsing, C. H.; Lin, M. C.; Choi, P. C.; Huang, W. C.; Kai, J. I.; Tsai, C. C.; Cheng, Y. L.; Hsieh, C. Y.; Wang, C. Y.; Chang, Y. P.; Chen, Y. H.; Chen, C. L.; Lin, C. F. Anesthetic propofol reduces endotoxic inflammation by inhibiting reactive oxygen species-regulated Akt/IKKbeta/NF-kappaB signaling. *PLoS One* **2011**, *6*, e17598.
(53) Dai, Y.; Chen, S.; Wang, L.; Pei, X. Y.; Funk, V. L.; Kramer, L. B.; Dent, P.; Grant, S. Disruption of IkappaB kinase (IKK)-mediated RelA serine 536 phosphorylation sensitizes human multiple myeloma cells to histone deacetylase (HDAC) inhibitors. *J. Biol. Chem.* **2011**, *286*, 34036−50.
(54) Frakes, A. E.; Ferraiuolo, L.; Haidet-Phillips, A. M.; Schmelzer, L.; Braun, L.; Miranda, C. J.; Ladner, K. J.; Bevan, A. K.; Foust, K. D.; Godbout, J. P.; Popovich, P. G.; Guttridge, D. C.; Kaspar, B. K. Microglia induce motor neuron death via the classical NF-kappaB pathway in amyotrophic lateral sclerosis. *Neuron* **2014**, *81*, 1009−23.
(55) Kobayashi, E. H.; Suzuki, T.; Funayama, R.; Nagashima, T.; Hayashi, M.; Sekine, H.; Tanaka, N.; Moriguchi, T.; Motohashi, H.; Nakayama, K.; Yamamoto, M. Nrf2 suppresses macrophage inflammatory response by blocking proinflammatory cytokine transcription. *Nat. Commun.* **2016**, *7*, 11624.

DOI: 10.1021/acs.jafc.8b00437
J. Agric. Food Chem. 2018, 66, 5790−5801